Journal of Neurodevelopmental Cognition

Journal of Neurodevelopmental Cognition 6(3) (2025) 1- 10 10.48308/jncog.2026.244436.1038
ISSN: 2645-565X
http://www.jncog.sbu.ac.ir

# Alpha-band fronto-posterior imaginary coherence during musical joint action: null results from an open EEG dataset

Mohammad Mahdi Rezapour*[1]

[1] *Institute for Cognitive and Brain Sciences, Shahid Beheshti University, Tehran, Iran*

**Abstract**

**Objective**: Joint agency–the experience of controlling action outcomes together with another person–is a core construct in social cognition. We reanalyzed the open Joint Agency EEG dataset (N = 23 for condition contrast; N = 21 for rating split) to test whether intra-brain alpha-band (8–13 Hz) connectivity supports this experience.

**Method:** Specifically, we estimated seed-based imaginary coherence from frontal electrode Fz_L to distributed scalp channels. Building on prior work linking auditory ERPs and inter-brain beta synchrony to joint agency, we tested two contrasts: (1) objective task condition (musical duet/joint vs constant-pitch/individual) and (2) subjective experience (within-subject median split of JointAgencyRatings: high vs low). Subject-level maps were compared using cluster-based one-sample permutation tests with channel-adjacency correction.

**Results:** In both analyses, no clusters survived correction ($p < .05$). Although descriptive topographies showed spatially structured variation, effects were not statistically reliable at the cluster level.

**Discussion**: These null results provide informative constraints on alpha-gating accounts of joint agency. Practically, they suggest that future studies should test alternative mechanisms, time windows, and network targets when probing neural signatures of shared agency.

* Corresponding author

*Email addresses: mohammadrezapour15@gmail.com*

*Received: July 2025* *Accept: August 2025*

**Keywords**: joint agency, alpha oscillations, imaginary coherence, EEG, social cognition, open data

## 1. Introduction

Joint agency refers to the experience that "we" are causing an action outcome together, rather than each person acting alone. As a metacognitive and phenomenological component of social interaction, it is central to how humans coordinate behavior, assign responsibility, and represent shared intentions in cooperative contexts (Loehr, 2022). In social cognitive neuroscience, joint agency is especially valuable because it links first-person experience to measurable interpersonal dynamics. It is shaped by sensorimotor contingencies and by higher-level beliefs about shared goals and partner contributions. Behavioral evidence further shows that perceived joint agency is not reducible to simple temporal synchrony; relational structure between partners also matters (Zhou et al., 2023).

An important contribution in this area is Zhou's (2025) doctoral dissertation, which analyzed the same open EEG hyperscanning dataset used here. That work reported joint-agency-related modulation of intra-brain auditory event-related potentials and inter-brain beta synchrony. These findings demonstrated that both individual sensory processing and interpersonal neural coordination contribute to shared control experiences. However, intra-brain alpha-band functional connectivity was not directly tested.

This gap limits mechanistic understanding. Alpha oscillations (8–13 Hz) are strongly implicated in top-down attentional control, information selection, and large-scale cortical communication (Klimesch, 2012; Nunez et al., 2001). Fronto-posterior coherence has also been associated with executive control processes in demanding cognitive tasks (Sauseng et al., 2005). Among candidate rhythms, alpha is therefore a plausible mechanism for coordinating attention, sensorimotor predictions, and control signals during shared action. If joint agency depends partly on controlled access to self- and partner-related information, alpha-band coupling should be a relevant target for testing that mechanism.

Methodologically, connectivity inference in EEG requires guarding against spurious coupling from volume conduction. The imaginary component of coherency reduces zero-lag effects likely driven by source spread (Nolte et al., 2004), providing a conservative estimate of functional interaction. Applying this measure to the joint agency dataset allows extension of prior findings beyond ERPs and inter-brain beta synchrony to within-brain network communication.

Accordingly, this Brief Report tested whether joint agency modulates seed-based alpha-band imaginary coherence from Fz_L to distributed scalp channels. Two hypotheses were evaluated: (a) musical duet (joint) trials would show stronger Fz-seeded alpha-band imaginary coherence across distributed scalp channels than constant-pitch (individual) trials, and (b) high perceived joint-agency trials would show stronger coherence than low perceived joint-agency trials. Using an open dataset and reproducible analysis pipeline, we aimed to refine mechanistic accounts of shared agency by testing a theoretically motivated but previously unexamined neural marker.

## 2. Method

### Dataset

Raw data were obtained from the Joint agency EEG dataset (OpenNeuro ds007471; https://doi.org/10.18112/openneuro.ds007471.v1.0.0; CC0). The dataset contains 32 pairs (sub-01 to sub-32); sub-05 was excluded because no EEG file was available. EEG was recorded in BrainVision format (.eeg/.vhdr/.vmrk), with channels 1–32 corresponding to the left participant and channels 33–64 to the right participant. SamplingInterval was 1000 microseconds (1000 Hz).

Each participant contributed 40 task trials in total, comprising 20 duet (joint) and 20 constant-pitch (individual) trials, organized as four duet blocks and four constant blocks with five trials per block.

### Preprocessing

Analyses were restricted to left-participant channels (suffix _L). Data were band-pass filtered (1–40 Hz), resampled to 250 Hz, and epoched from -0.5 to 1.0 s relative to trial onset, with baseline correction from -0.2 to 0 s. Artifact rejection used a peak-to-peak threshold of 200 microvolts (relaxed threshold). No additional re-referencing step was applied in the preprocessing scripts. Dataset metadata list the acquisition EEG reference as left mastoid. ICA or other component-based ocular/muscle artifact correction was not applied in the primary pipeline. Rejection was applied automatically during epoch construction using a fixed MNE peak-to-peak criterion (reject={"eeg": 200e-6}). Across participants with available EEG files and generated epoch outputs (31 subjects; 40 candidate trials each), the mean rejected-epoch proportion was 73.7%. This relatively high rejection rate likely reflects the conservative peak-to-peak artifact threshold applied during epoch construction. Subsequent trial-equalization procedures further reduced the number of trials available for group analyses but did not contribute to artifact rejection itself.

All preprocessing and analysis were performed in Python 3.14 using MNE-Python (version 1.12.1); connectivity estimation used MNE-Connectivity (version 0.8.1).

Filtering used MNE's zero-phase FIR implementation (forward-backward application; firwin design), with automatically selected filter length and transition bandwidth parameters as provided by the MNE defaults for the specified 1–40 Hz passband.

### Trial definition and selection

Trial onsets were identified using the validated trial-marking procedure described in the analysis pipeline: S107 markers defined block boundaries, S105 markers indexed trial starts, and S1 indicated the beginning of the test segment when present. Eight analyzed blocks were retained, and five task-relevant starts were selected per block, yielding 40 trials per subject. Behavioral labels were assigned using the left-participant behavioral records indexed by TrialNumber. ExperimentalCondition values (1 = joint, 0 = individual) were then used to assign trial labels, and trials were retained and balanced within each subject to maximize usable data while matching condition counts.

The epoch window (-0.5 s to +1.0 s relative to trial onset) was selected to capture both the pre-cue baseline period and the early post-onset interval in which agency-related processes may emerge. Baseline correction from -0.2 to 0 s was applied to remove pre-stimulus offsets before connectivity estimation. It remains possible that joint-agency effects unfold later or within narrower temporal intervals; therefore, the present broad window may dilute transient effects, and future work should use time-frequency-resolved or sliding-window connectivity analyses to isolate more specific time periods.

JointAgencyRatings were self-reported on a 1–7 scale and were collected after each trial, consistent with the dataset event documentation indicating that S106 marks trial end after completion of rating scales. Ratings were aligned to the 40 left-participant trials via TrialNumber indexing. A within-subject median split was then applied, with ratings strictly greater than the participant-specific median labeled High agency and ratings at or below the median labeled Low agency.

**Connectivity analysis**

Imaginary coherence (imcoh) was computed between seed electrode Fz_L and scalp channels using spectral_connectivity_epochs (fmin = 8 Hz, fmax = 13 Hz, faverage = True, multitaper). Vertical and horizontal EOG channels and the reference channel were excluded before topographic inference, leaving 27 scalp EEG channels. Condition trial counts were equalized by random subsampling to the within-subject minimum using numpy.random.default_rng with a fixed seed of 42. A single random subsampling draw was used for the main analysis. The stability of the random subsampling procedure across alternative random seeds was not formally evaluated. Although the use of a fixed random seed ensures reproducibility of the present analysis, future work should examine robustness across multiple subsampling iterations to verify that the observed null findings are not dependent on a particular random draw. Subjects with fewer than two equalized trials per condition were excluded from group analyses.

Fz was selected as the sole seed because it overlies medial frontal cortex, a region strongly implicated in action monitoring, cognitive control, and self-related processing. Prior work on joint action and joint agency has similarly highlighted medial prefrontal involvement (Shiraishi & Shimada, 2021). Using a single, theoretically motivated seed also reduces the multiple-comparison burden that would arise from testing all electrodes as candidate seeds and enables a focused hypothesis about fronto-posterior communication.

For spectral estimation, multitaper connectivity was computed with the default MNE-Connectivity settings for spectral_connectivity_epochs unless otherwise specified.

**Statistical analysis**

Group-level contrasts were tested with one-sample cluster-based permutation tests (mne.stats.permutation_cluster_1samp_test) applied to subject-wise difference maps. Channel adjacency was estimated from sensor geometry, and cluster formation used a two-sided t-threshold at $p < 0.05$ with degrees of freedom equal to $n - 1$. Cluster significance was evaluated with 5000 permutations.

All tests were two-tailed, and the cluster-forming threshold was derived from the t-distribution at alpha = 0.05 with degrees of freedom n - 1 for each contrast; cluster-level significance was then assessed with 5000 permutations.

The final sample sizes (N = 23 for the condition contrast and N = 21 for the rating split) were determined after preprocessing, quality-control exclusion, and trial equalization procedures, and therefore statistical power to detect small effects may have been limited.

## 3. Results

In the objective condition contrast (Joint vs Individual), group analysis included 23 subjects after quality-control exclusions. Excluded subjects were sub-04, sub-07, sub-10, sub-16, sub-18, sub-19, sub-24, and sub-25 (fewer than two equalized trials per condition). The statistical map was based on 27 scalp channels and used a cluster-forming threshold of t = 2.073873 (df = 22). No clusters survived cluster-level correction. Numerically, the corresponding connectivity arrays had shape (23, 27).

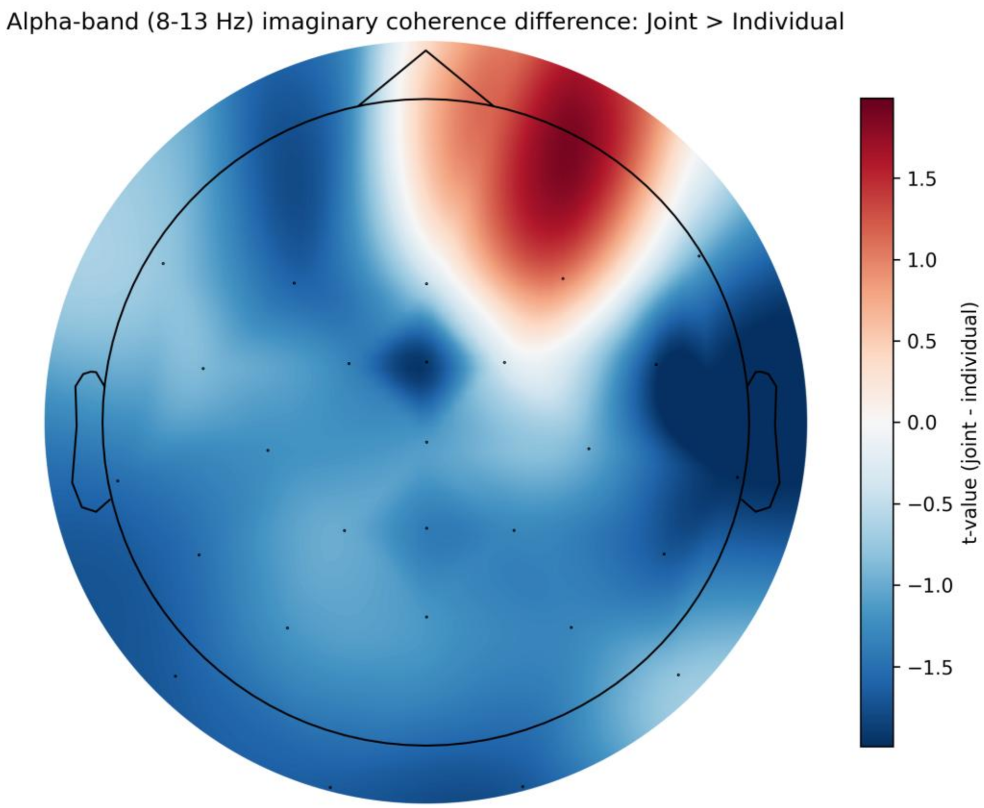


***Figure 1**. Topographic map of t-values for the Joint > Individual alpha-band imaginary coherence contrast. Positive t-values indicate stronger coherence in the Joint condition. No electrodes survived cluster-level correction (p < 0.05, cluster-based permutation test).*

In the subjective rating contrast (High vs Low JointAgencyRatings), 21 subjects met inclusion criteria, with a cluster-forming threshold of t = 2.085963 (df = 20) across the same 27-channel set. Excluded subjects were sub-04, sub-07, sub-14, sub-16, sub-19, sub-20, sub-24, sub-25, sub-30, and sub-32 (fewer than two equalized trials per condition). Again, no clusters survived correction. The corresponding connectivity arrays had shape (21, 27). Thus, corrected inference did not support reliable condition effects in either objective or subjective contrasts. Nevertheless, the topographies showed visible but non-significant spatial variation, with localized positive and negative regions that did not reach cluster significance.

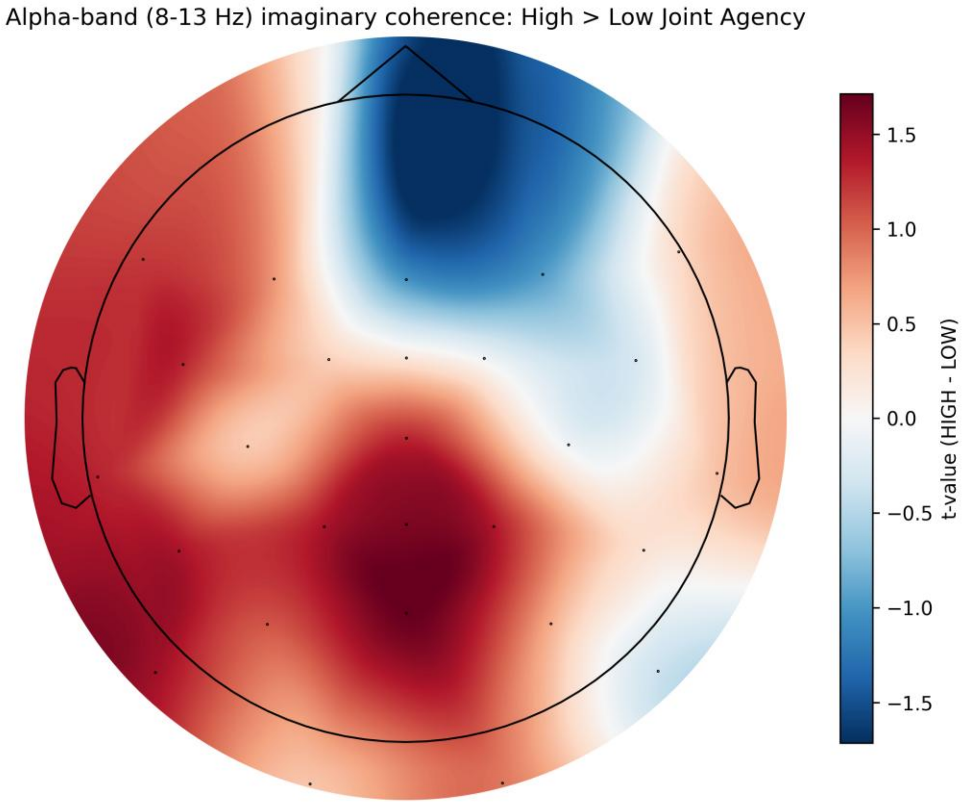


*Figure 2. Topographic map of t-values for the High > Low perceived joint agency alpha-band imaginary coherence contrast. Positive t-values indicate stronger coherence in the High-rating condition. No electrodes survived cluster-level correction (p < 0.05, cluster-based permutation test).*

| Subject ID | Condition Contrast (exclusion reason) | Rating Split (exclusion reason) |
|---|---|---|
| sub-04 | Excluded (<2 equalized trials per condition) | Excluded (<2 equalized trials per condition) |
| sub-07 | Excluded (<2 equalized trials per condition) | Excluded (<2 equalized trials per condition) |
| sub-10 | Excluded (<2 equalized trials per condition) | Included |
| sub-14 | Included | Excluded (<2 equalized trials per condition) |

| | | |
|---|---|---|
| sub-16 | Excluded (<2 equalized trials per condition) | Excluded (<2 equalized trials per condition) |
| sub-18 | Excluded (<2 equalized trials per condition) | Included |
| sub-19 | Excluded (<2 equalized trials per condition) | Excluded (<2 equalized trials per condition) |
| sub-20 | Included | Excluded (<2 equalized trials per condition) |
| sub-24 | Excluded (<2 equalized trials per condition) | Excluded (<2 equalized trials per condition) |
| sub-25 | Excluded (<2 equalized trials per condition) | Excluded (<2 equalized trials per condition) |
| sub-30 | Included | Excluded (<2 equalized trials per condition) |
| sub-32 | Included | Excluded (<2 equalized trials per condition) |
| sub-05 | Excluded (EEG data file unavailable; no .eeg file in dataset) | Excluded (EEG data file unavailable; no .eeg file in dataset) |

Effect size and power analysis

To quantify sensitivity, we estimated peak-channel effect sizes for channels showing the largest numerical differences in the topographies. Peak t-values were approximately at the cluster-forming range (~2.07–2.09), corresponding to Cohen's $d \approx 2.07/\text{sqrt}(23) \approx 0.43$ for the condition contrast and $d \approx 2.09/\text{sqrt}(21) \approx 0.46$ for the rating split. These values are peak-channel estimates only and should not be interpreted as global effect sizes. Post-hoc power was estimated analytically using the noncentral t distribution for a one-sample two-tailed t test (alpha = 0.05), indicating that approximately 34 analyzable participants would be required to achieve 80% statistical power to detect a medium effect (Cohen's d = 0.5). The current sample sizes (N = 23 and N = 21) are therefore underpowered for small-to-medium effects. Accordingly, the present null findings constrain large effects but do not rule out smaller, potentially meaningful, alpha-band connectivity changes.

## 4. Discussion

Across both contrasts, the analyses did not show evidence of robust enhancement in cue-locked Fz-seeded alpha-band imaginary coherence across distributed scalp channels. This outcome places meaningful constraints on strong versions of alpha-gating accounts that predict a clear increase in frontal-to-posterior coupling during joint agency. More specifically, the present data suggest that if alpha contributes to shared agency, its effects are likely subtle, context-dependent, or temporally distributed beyond the tested epoch window. The descriptive topographic gradients indicate structured variation, but those patterns were not reliable after correction for multiple comparisons.

However, the absence of significant cluster-corrected effects does not imply that alpha-band connectivity plays no role in joint agency. Null findings in a moderate sample must be interpreted cautiously; they constrain strong claims but do not disprove more subtle involvement of fronto-posterior alpha coupling. Methodological factors such as sample size, the specific seed location, and the time window examined all limit the sensitivity of the current analysis.

This null result is consistent with Zhou (2025), who found joint-agency effects in ERPs and inter-brain beta synchrony but not in intra-brain connectivity, and with Gregory et al. (2022), who reported theta-band rather than alpha-band differences during social attention. Bayesian multilevel models or Bayesian paired ROI analyses may provide a stronger framework for quantifying evidence for both null and alternative hypotheses in future analyses.

More specifically, Zhou (2025) reported joint-agency-related modulation of auditory ERP components (including N1 and P2), indicating modulation of early sensory processing under shared control. In contrast, the present null findings suggest that this agency-related modulation may not extend to sustained Fz-seeded alpha-band coupling across distributed scalp channels in the same task context. This dissociation indicates that ERP amplitude and connectivity may capture distinct facets of joint agency, and is consistent with evidence that inter-brain synchrony is also relevant during cooperative action (see also Shiraishi & Shimada, 2021), suggesting that inter-brain and intra-brain metrics may index partially distinct processes. Together with Gregory et al. (2022), who reported theta but not alpha effects in social attention, the current findings reinforce the interpretation that alpha is not necessarily the primary carrier of social-attentional modulation in this paradigm class. Previous EEG studies have demonstrated that fronto-parietal coherence can index distributed executive-control processes (Sauseng et al., 2005), suggesting that coherence measures are capable of capturing large-scale functional coupling under appropriate task conditions. In this context, Zhou's ERP findings can coexist with the near-zero alpha-connectivity effects observed here: ERP amplitudes primarily index local, phase-locked sensory processing, whereas alpha imaginary coherence indexes distributed non-zero-lag functional network coupling. This distinction provides a plausible mechanistic basis for dissociation while remaining consistent with inter-brain synchrony findings (Shiraishi & Shimada, 2021).

Several limitations should be acknowledged. First, sample size was reduced after equalization and quality-control exclusion, which may have limited sensitivity to small effects. In addition, the relatively stringent artifact-rejection procedure substantially reduced the number of analyzable epochs, potentially decreasing statistical sensitivity to subtle connectivity effects. At 80% power for a two-tailed one-sample t-test (alpha = 0.05), the minimum detectable effect size is approximately $d \approx 0.59$ for $N = 23$ and $d \approx 0.62$ for $N = 21$. Effects smaller than these thresholds could not be reliably detected, which represents a meaningful Type II error risk in the present analyses. Future studies should pre-register a target effect size and recruit sample sizes accordingly. Second, the seed-based design centered on Fz_L, and alternative seed choices could capture different control-network configurations. Third, the analysis focused on the 8–13 Hz alpha band; effects may emerge in other frequencies or in cross-frequency coupling. Finally, agency-related dynamics may be more detectable in other network architectures, including inter-brain connectivity, than in the present intra-brain contrast framework. Future work should examine whether alpha-band fronto-posterior connectivity is instead modulated by real-time social gaze cues (as in joint-attention paradigms) or whether it operates primarily at the inter-brain level during shared intentionality.

An additional limitation concerns statistical power given the final sample sizes (N = 23 and N = 21). Smaller samples reduce power to detect subtle effects, and cluster-based permutation testing—while appropriately controlling multiple comparisons—still requires sufficiently large effects to survive correction. Therefore, the current null findings do not rule out smaller alpha-band connectivity changes that may be detectable in larger samples.

## 5. Conclusion

This null finding provides informative constraints on alpha-gating accounts of joint agency and suggests that future studies explore alternative neural markers and paradigms.

### Data Availability and Supplementary Data

The raw dataset is openly available on OpenNeuro (ds007471, https://doi.org/10.18112/openneuro.ds007471.v1.0.0) under a CC0 license. All analysis scripts and derived epoch/connectivity files are available in the project archive and will be deposited in public OSF and GitHub repositories for open access.

## Acknowledgment

We thank the creators of the Joint Agency EEG dataset for making their data openly available.

### References

Baxter, M. G., & Burwell, R. D. (2017). Promoting transparency and reproducibility in Behavioral Neuroscience: Publishing replications, registered reports, and null results. Behavioral Neuroscience, 131(4), 275–276. https://doi.org/10.1037/bne0000207

Gregory, S. E. A., Wang, H., & Kessler, K. (2022). EEG alpha and theta signatures of socially and non-socially cued working memory in virtual reality. Social Cognitive and Affective Neuroscience, 17(6), 531–540. https://doi.org/10.1093/scan/nsab123

Klimesch, W. (2012). Alpha-band oscillations, attention, and controlled access to stored information. Trends in Cognitive Sciences, 16(12), 606–617. https://doi.org/10.1016/j.tics.2012.10.007

Loehr, J. D. (2022). The sense of agency in joint action: An integrative review. Psychonomic Bulletin & Review, 29(4), 1089–1117. https://doi.org/10.3758/s13423-021-02051-3

Nolte, G., Bai, O., Wheaton, L., Mari, Z., Vorbach, S., & Hallett, M. (2004). Identifying true brain interaction from EEG data using the imaginary part of coherency. Clinical Neurophysiology, 115(10), 2292–2307. https://doi.org/10.1016/j.clinph.2004.04.029

Nunez, P. L., Wingeier, B. M., & Silberstein, R. B. (2001). Spatial-temporal structures of human alpha rhythms: Theory, microcurrent sources, multiscale measurements, and global binding of local networks. Human Brain Mapping, 13(3), 125–164. https://doi.org/10.1002/hbm.1030

Özel, P. (2024). Dynamic neural network states during social and non-social cueing in virtual reality working memory tasks: A LEiDA approach. Brain Sciences, 15(1), 4. https://doi.org/10.3390/brainsci15010004

Sauseng, P., Klimesch, W., Schabus, M., & Doppelmayr, M. (2005). Fronto-parietal EEG coherence in theta and upper alpha reflect central executive functions of working memory. International Journal of Psychophysiology, 57(2), 97–103. https://doi.org/10.1016/j.ijpsycho.2005.03.018

Shiraishi, M., & Shimada, S. (2021). Inter-brain synchronization during a cooperative task reflects the sense of joint agency. Neuropsychologia, 154, 107770. https://doi.org/10.1016/j.neuropsychologia.2021.107770

Zhou, Z. (2025). Cognitive and neural mechanisms underlying the sense of joint agency during joint actions [Doctoral dissertation, University of Saskatchewan].

Zhou, Z., Christensen, J., Cummings, J. A., & Loehr, J. D. (2023). Not just in sync: Relations between partners' actions influence the sense of joint agency during joint action. Consciousness and Cognition, 111, 103521. https://doi.org/10.1016/j.concog.2023.103521

Zhou, Z., Zamm, A., Christensen, J., Rao, V., & Loehr, J. D. (2026). Joint agency EEG dataset [Data set]. OpenNeuro. https://doi.org/10.18112/openneuro.ds007471.v1.0.0